Clinical Nutrition 53 (2025) 99–108

Contents lists available at ScienceDirect

Clinical Nutrition

journal homepage: http://www.elsevier.com/locate/clnu

Randomized Control Trials

Serum Galectin-9 and Decorin in relation to brain aging and the green-Mediterranean diet: A secondary analysis of the DIRECT PLUS randomized trial

Dafna Pachter [a,1], Anat Yaskolka Meir [a,b,1], Alon Kaplan [a], Gal Tsaban [a,c], Hila Zelicha [a], Ehud Rinott [a], Gidon Levakov [d], Ofek Finkelstein [d], Ilan Shelef [a,c], Moti Salti [e], Frauke Beyer [f], Veronica Witte [f], Nora Klöting [g], Berend Isermann [h], Uta Ceglarek [h], Tammy Riklin Raviv [i], Matthias Blüher [g], Michael Stumvoll [g,j], Dong D. Wang [b], Frank B. Hu [b,k,l], Meir J. Stampfer [b,k,l], Galia Avidan [e,**], Iris Shai [a,g,k,m,*]

[a] The Health & Nutrition Innovative International Research Center, Faculty of Health Sciences, Ben-Gurion University of the Negev, David Ben-Gurion Blvd. 1, Beer-Sheva, 8410501, Israel
[b] Department of Epidemiology, Harvard T.H. Chan School of Public Health, 677 Huntington Avenue, Boston, MA 02115, USA
[c] Soroka University Medical Center, Rager Boulevard, Beer-Sheva, 84101, Israel
[d] Department of Cognitive and Brain Sciences and The School of Brain Sciences and Cognition, Ben-Gurion University of the Negev, David Ben-Gurion Blvd. 1, Beer-Sheva 8410501, Israel
[e] Department of Psychology, Ben-Gurion University of the Negev, David Ben-Gurion Blvd. 1, Beer-Sheva 8410501, Israel
[f] Department of Neurology, Max-Planck-Institute for Human Cognitive and Brain Sciences, and Cognitive Neurology, University of Leipzig Medical Center, Leipzig, Stephanstraße 1A, D-04103 Leipzig Germany
[g] Helmholtz Institute for Metabolic, Obesity and Vascular Research (HI-MAG), Helmholtz Zentrum München, University of Leipzig and University Hospital Leipzig, Philipp-Rosenthal-Straße 27, 04103 Leipzig, Germany
[h] Institute of Laboratory Medicine, Clinical Chemistry, and Molecular Diagnostics, University of Leipzig Medical Center, Paul-List-Straße 13/15, 04103 Leipzig, Germany
[i] The School of Electrical and Computer Engineering, Ben Gurion University of the Negev, David Ben-Gurion Blvd. 1, Beer-Sheva 8410501, Israel
[j] Medical Department III – Endocrinology, Nephrology, Rheumatology, University of Leipzig, Medical Center, Liebigstraße 20, Haus 4, Leipzig, 04103, Germany
[k] Department of Nutrition, Harvard T.H. Chan School of Public Health, 665 Huntington Avenue, Boston, MA 02115, USA
[l] Channing Division of Network Medicine, Department of Medicine, Brigham and Women's, Hospital and Harvard Medical School, 181 Longwood Avenue, Boston, MA 02115, USA
[m] School of Sustainability, Reichman University, Israel

ARTICLE INFO

Article history:
Received 29 April 2025
Accepted 8 August 2025

Keywords:
Brain age
Proteomics
Randomized controlled trial

SUMMARY

Background and aims: We explored whether changes in serum proteomic profiles differed between participants with distinct brain aging trajectories, and whether these changes were influenced by dietary intervention.
Methods: In this secondary analysis of the 18-month DIRECT PLUS trial, 294 participants were randomized to one of three arms: 1) Healthy dietary guidelines (HDG); 2) Mediterranean (MED) diet (+440 mg/day polyphenols from walnuts); or 3) low red/processed meat green-MED diet (+1240 mg/day polyphenols from walnuts, Mankai plant, and green tea). We measured 87 serum proteins (Olink-CVDII). We used Magnetic-Resonance-Imaging (MRI)-assessed 3D-T1-weighted brain scans for brain age

Abbreviations: AD, Alzheimer disease; ALKP, alkaline phosphatase; ALT, alanine transaminase; BAG, Brain age gap; BMI, body mass index; BP, Blood pressure; CNN, convolutional neural network; CRP, C-reactive protein; CSF, cerebral-spinal fluid; CVD, cardiovascular disease; DCN, Decorin; ECM, extracellular matrix; FDR, false discovery rate; Gal-9, Galectin 9; green-MED diet, Mediterranean diet higher in polyphenols and lower in red/processed meat; HbA1c, Hemoglobin A1c; HDG, Healthy dietary guidelines; HDLc, High-density lipoprotein cholesterol; HOC, Hippocampal Occupancy Score; IQR, Interquartile Range; LDLc, Low-density lipoprotein cholesterol; LVV, lateral ventricle volume; MCI, Mild cognitive impairment; MED, Mediterranean diet; MRI, Magnetic-Resonance-Imaging; NPX, normalized protein expression; PA, Physical activity; PCA, principal component analysis; PEA, proximity extension assay; RMSE, root mean square error; TG, Triglyceride; WC, Waist circumference.

* Corresponding author. The Health & Nutrition International Research Center, School of Public Health, Faculty of Health Sciences, Ben-Gurion University of the Negev, P. O. Box 653, Beer Sheva 84105, Israel.
** Corresponding author. Department of Psychology, Ben-Gurion University of the Negev, Beer Sheva, Israel.
E-mail addresses: galiaa@bgu.ac.il (G. Avidan), irish@bgu.ac.il (I. Shai).
[1] These authors contributed equally to this work.

https://doi.org/10.1016/j.clnu.2025.08.021

Dietary interventions
Peripheral protein expression

calculation (by convolutional neural network) to identify protein markers reflecting the brain age gap (BAG; deviation of MRI-assessed brain age from chronological age).
Results: At baseline, lower weight, waist circumference, diastolic blood pressure, and HbA1c parameters were associated with a younger brain age than expected. Specifically, higher levels of two proteins, Galectin-9 (Gal-9) and Decorin (DCN), were associated with accelerated brain aging (larger BAG). A proteomics principal component analysis (PCA) revealed a difference in PC1 between the two time-points for participants with accelerated brain aging. Between baseline and 18 months, Gal-9 significantly decreased among individuals who completed the intervention with attenuated brain aging, while DCN significantly increased among those who completed the trial with accelerated brain aging. A significant interaction was observed between the green-MED diet and proteomics PCA, resulting in a beneficial change compared to the HDG. Participants in the green-MED diet significantly decreased Gal-9 compared to the HDG diet and from baseline.
Conclusions: Higher serum levels of Gal-9 and DCN may indicate an acceleration of brain aging and could be reduced by a green-MED/high-polyphenol (green tea and Mankai) and low-red/processed meat diet.
Trial registration number: NCT03020186.

1. Introduction

Age-related neurodegenerative conditions are often characterized by reduced brain volume (atrophy), as well as enlargement of ventricles and cerebral spinal fluid (CSF) spaces [1]. However, these changes do not always correspond with chronological age. Factors such as diabetes, inflammation, hypertension, high cholesterol, and accumulation of β-amyloid and tau markers can accelerate brain aging [2–10].

In recent years, brain age has emerged as a promising index of overall brain health [10–13]. Brain age estimation is commonly performed by predicting age from neuroimaging data in a healthy reference population and applying the trained model to an independent, previously unseen subject [14]. The brain age gap (BAG) is defined as the difference between an individual's brain age based on an MRI scan and their chronological age. A positive BAG reflects brain age higher than chronological age or accelerated brain aging. In contrast, a negative BAG indicates brain age lower than chronological age or attenuated brain aging [15]. Higher brain age, in relation to chronological age, is observed in various neurological conditions, including mild cognitive impairment (MCI) and Alzheimer's disease (AD). However, to date, there is limited evidence supporting the use of circulating proteomic markers as indicators of BAG.

Recently, in the 18-month DIRECT PLUS trial, we found that a green-MED (high-polyphenol) diet, rich in Mankai, green tea, and walnuts and low in red/processed meat, is potentially neuroprotective for age-related brain atrophy [16]. In a sub-study of this trial, we also demonstrated that lower consumption of processed food, sweets, and beverages was associated with attenuated brain age based on resting-state functional MRI [17]. The current study is a secondary analysis of the DIRECT PLUS trial. We used cross-sectional and longitudinal data from this trial to identify circulating proteomic signatures reflecting BAG status at baseline and at 18 months, and the impact of lifestyle interventions on these proteomic signatures. Our primary objective was to examine whether changes in circulating proteomic profiles over the 18-month intervention period differed between participants with distinct brain aging trajectories (as defined by BAG patterns), and to explore the effect of lifestyle intervention on these changes.

2. Methods

2.1. Study recruitment

The 18-month DIRECT PLUS trial (ClinicalTrials.gov Identifier: NCT03020186) included 294 participants and was conducted in an isolated workplace (Nuclear Research Center Negev, Dimona, Israel). The inclusion criteria were age ≥30 years with abdominal obesity (waist circumference (WC): men>102 cm, women >88 cm) or dyslipidemia (triglycerides>150 mg/dL; high-density lipoprotein cholesterol (HDLc) ≤40 mg/dL for men, ≤50 mg/dL for women) (Exclusion criteria are detailed in Supplementary Methods 1). The study was approved by the Institutional Review Board at Soroka University Medical Center (SOR-0280-16). The trial was conducted in a single phase over an 18-month period from May 2017 to November 2018. Participants provided written informed consent and did not receive compensation for their participation.

2.2. Study design, randomization, and intervention

Participants were randomly assigned, using a computer-generated random allocation sequence, in a 1:1:1 ratio to one of three intervention groups: 1) HDG, an active control group; 2) a traditional calorie-restricted Mediterranean (MED) diet, low in simple carbohydrates; or 3) the green-MED diet. We conducted the randomization in a single phase, with a parallel assignment intervention model, and participants were aware of their assigned intervention (open-label protocol). Allocation concealment was maintained by revealing the group assignment only after participant eligibility and consent were confirmed. The first participant was enrolled on January 28, 2017, and the last participant was enrolled on April 30, 2017. The trial was initiated and conducted in a single phase between May 2017 and November 2018 (For enrollment and randomization rules, please see Supplementary Fig. 1.) [18]. Each group received specific nutritional guidance along with physical activity (PA) instructions. The HDG group received basic health-promoting dietary guidelines. The MED group received guidelines for a calorie-restricted traditional MED

diet, low in simple carbohydrates, as described in our previous papers [19,20].

The MED diet was rich in vegetables, with beef and lamb replaced by poultry and fish. Both MED diets included 28 g of walnuts per day. The green-MED diet, in addition to 28 g of walnuts per day, was lower in processed and red meat compared to the MED diet and richer in plants and polyphenols. This was achieved through the consumption of 3–4 cups of green tea and 500 ml of a Mankai-based (cultivated duckweed) product daily [21–23], a green shake at dinner. Both MED diets were equally calorie-restricted, with 1500–1800 kcal/day for males and 1200–1400 kcal/day for females. All participants were provided with free gym membership and PA guidelines. Additionally, they attended periodic 90-min nutritional and PA sessions at their workplace, facilitated by a multidisciplinary team of physicians, clinical dietitians, and fitness instructors. Guidelines, characteristics of the study population, and adherence to the dietary and physical activity interventions were previously reported in detail in our prior publication [18], and further elaborated in Supplementary Methods 2.

2.3. Clinical measurements

Clinical and anthropometric biomarkers were measured at baseline and after 18 months. Height was measured to the nearest millimeter using a standard wall-mounted stadiometer. Body weight was measured in the morning after an overnight fast, with participants wearing light clothing and no shoes, to the nearest 0.1 kg, using the same calibrated scale for all participants. All measurements were performed by trained trial staff and not self-reported. WC was measured halfway between the lowest rib and the iliac crest to the nearest millimeter using standard procedures and an anthropometric measuring tape. Two blood pressure (BP) and heart rate measurements were recorded after resting using an automatic BP monitor, and BP was calculated as the mean of the two measurements. Blood samples were taken at 8 am after a 12-h fast, and aliquots were frozen for later assays (Further laboratory methods are detailed in Supplementary Methods 3).

2.4. Proteomic panel

We assayed available serum samples for proteomic analysis from baseline (N = 211) and 18-months (N = 208), focusing on participants with complete data at baseline and after the 18-month intervention. The protein analysis was conducted on 92 proteins with Olink's CARDIOVASCULAR II panel on their proteomics platform. Five proteins with more than 5 % missing data (BNP, ITGB1BP2, PARP1, SERPINA12, STK4) were excluded. The proteomics platform uses proximity extension assay (PEA) technology in a 96-well plate format. Each panel contains 92 pairs of oligonucleotide-labeled antibody probes that attach to their target proteins in serum. Following a proximity-dependent DNA polymerization event, a PCR reporter sequence is created, amplified, and measured using real-time PCR. Internal and external controls are employed for data normalization and quality assurance. Intra- and inter-coefficient variance (CV)% were calculated from control samples (pooled plasma samples) included on each plate. This platform provides data on normalized protein expression (NPX) using a log2 scale. More details about the Olink analysis are available in Supplementary Methods 4.

2.5. Brain MRI acquisition and brain age prediction

We analyzed eligible brain MRIs (216 at baseline and 18-m) for BAG calculation (Supplementary Fig. 1). MRI scans were conducted at the Soroka University Medical Center, Beer Sheva using a 3 T Philips Ingenia scanner (Amsterdam, The Netherlands) equipped with a standard head coil. High-resolution anatomical volumes were obtained using a T1-weighted 3D pulse sequence ($1 \times 1 \times 1$ mm^3, 150 slices, TR = 2500, TE = 30 ms, field of view $240 \times 220 \times 150$). Brain age was estimated using a previously validated convolutional neural network (CNN) model trained on external datasets, as described in detail in Supplementary Methods 5. The BAG was determined by calculating the difference in years between the predicted brain age and the chronological age.

2.6. Statistical analysis

The primary outcome, the BAG, was calculated at baseline and after 18 months as the residual from a linear regression model of predicted brain age on chronological age.

For the cross-sectional analysis, we stratified baseline characteristics by positive BAG values (indicating accelerated brain aging) versus negative (indicating attenuated brain aging). Continuous variables are presented as mean ± SD or median ± IQR, depending on their distribution, and as number (%) for categorical variables. Statistical tests used include Welch Two Sample t-test, Pearson's Chi-squared test, and Wilcoxon rank sum test. Spearman correlations were used to assess the associations between proteomics levels and BAG. Multiple testing was controlled using the false discovery rate (FDR) method, with a threshold set at 5 %. Partial correlations were calculated to adjust for age and sex. Elastic net regression with leave-one-out cross-validation (LOOCV) was used to establish proteomic scores to predict the BAG. Baseline data were used as training and test sets, and 18-month post-intervention data were used for validation.

For our primary longitudinal analysis, we conducted principal component analysis (PCA) on the full 87-protein panel within three distinct groups: the entire cohort, participants who completed the study with a positive BAG, and those with a negative BAG. Within each group, we applied a separate Linear Mixed Effects Model (LMM) to assess the change in the first principal component (PC1) between baseline and 18 months. Further, a volcano plot was applied to present differences in proteomic profiles for each BAG group. Then, we conducted a quantile regression of chronological age to test whether candidate protein levels were associated with chronological age across quantiles. In addition, we used LMM to test whether changes in PC1 over time differed by intervention group (time × group interaction).

Furthermore, we quantified the change in levels of specific proteins for each lifestyle intervention group by ANOVA after Bonferroni correction. In addition, separate LMMs were applied to compare the 18-month changes in protein markers from baseline, also adjusted for Bonferroni comparisons. Statistical analysis was performed using R (Version 4.2.0), details regarding the specific R packages used are provided in Supplementary Methods 6. Statistical significance was set at a two-sided alpha value of 0.05.

2.7. Ethics approval and consent to participate

The study was conducted in accordance with the Declaration of Helsinki, and the protocol was approved by the Medical Ethics

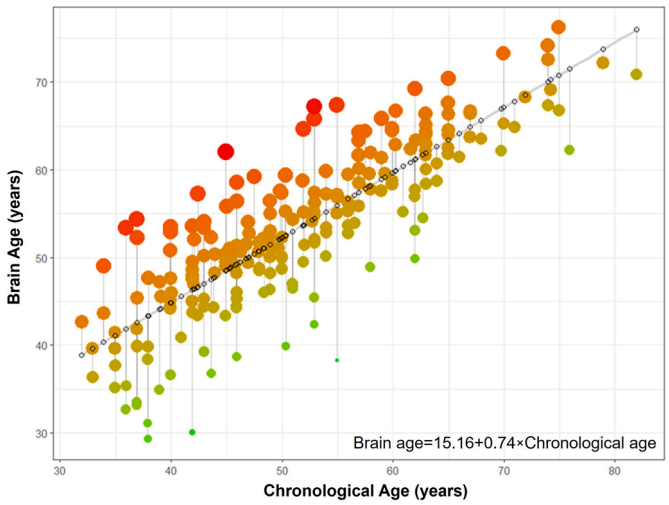

Fig. 1. Correlation of chronological age and brain age and Brain Age Gap representation. N = 216. Brain Age Gap (BAG) was determined by linear regression with brain age as the dependent variable and chronological age as the independent variable. BAG <0 represents delayed aging (expected brain age > observed brain age); BAG >0 represents accelerated aging (observed brain age > expected brain age). The color and size of the points indicate the magnitude of the residuals, with green and smaller dots showing smaller residuals and red and larger dots showing larger residuals.

Board and Institutional Review Board at Soroka University Medical Center, Be'er Sheva, Israel (SOR-0280-16). Participants provided written informed consent and received no compensation.

2.8. Role of funders

The study funders had no involvement in the design, data collection, analysis, interpretation, manuscript preparation, or submission for publication.

3. Results

3.1. Baseline characteristics of the participants

Chronological age and brain age were highly correlated (r = 0.82, p > 0.001; Fig. 1). Baseline characteristics of the 216 participants stratified by positive (accelerated brain aging-older brain than expected for their chronological age) and negative (attenuated brain aging-younger brain than expected for their chronological age) BAG are presented in Table 1. The mean BAG of the positive group (accelerated brain aging) was 4.0 ± 3.2 years, and for the negative group (attenuated brain aging), −4.2 ± 3.8 years. Participants with a younger brain age had a lower weight, WC, diastolic BP, and HbA1c (p < 0.05 for all).

3.2. Cross-sectional associations between proteomics and brain age gap at baseline

Baseline correlation analysis between BAG and 87 proteins of the proteomic panel revealed only two protein markers, Galectin 9 (Gal-9) and Decorin (DCN), both of which were significantly positively associated with greater BAG (FDR< 0.05; sex and age-adjusted) (of the 216 participants with BAG, we had proteomics available for 211; Fig. 2). In addition, we conducted stratified analyses within APOE-ε4 carriers (n = 33) and non-carriers (n = 172). Within each genotype subgroup, the associations of Gal-9 and DCN with BAG did not remain statistically significant after FDR correction. However, the correlation coefficients and their 95 % confidence intervals were comparable to those observed in the full cohort: for Gal-9, the full cohort showed r = 0.23 [0.093, 0.351], while non-carriers showed r = 0.18 [0.029, 0.321]; for DCN, the full cohort showed r = 0.22 [0.092, 0.350], and non-carriers showed r = 0.19 [0.042, 0.332]. These similarities suggest consistent associations, though the reduced statistical significance in the non-carrier subgroup may reflect lower power due to the smaller

Table 1
Baseline characteristics of the DIRECT PLUS participants stratified by delayed/accelerated brain aging[a].

	N	Delayed brain aging (BAG<0)	Accelerated brain aging (BAG>0)	p-value[b]
		N = 106	N = 110	
Age, years (range)	216	51.8 (32.9–82)	50.9 (31.9–74.9)	0.5
Brain age gap, years	216	−4.2 ± 3.8	4.0 ± 3.2	<0.001
Women	216	15 (14.2 %)	6 (5.5 %)	0.031
Weight, Kg	216	90.6 ± 12.2	95.2 ± 14.6	0.013
Height, cm	216	172.4 ± 8.6	173.5 ± 8.0	0.3
Waist circumference, cm	216	107.3 ± 7.0	111.2 ± 9.9	0.001
Systolic BP, mmHg	215	129.0 (118.5, 138.5)	130.0 (124.1, 138.5)	0.3
Diastolic BP, mmHg	215	78.0 (73.5, 85.5)	83.5 (75.6, 88.5)	0.016
Glucose, mg/dL	214	97.8 (92.5, 105.2)	98.5 (91.5, 106.8)	0.8
Fasting insulin, μU/mL	216	13.1 (10.1, 16.4)	12.8 (9.0, 18.4)	>0.9
HbA1c, μU/mL	216	5.3 (5.1, 5.6)	5.5 (5.2, 5.7)	0.046
Cholesterol, mg/dL	216	185.5 (164.6, 211.4)	194.8 (170.8, 211.5)	0.3
Triglycerides, mg/dL	216	131.4 (95.8, 175.0)	136.3 (100.2, 169.5)	>0.9
HDLc, mg/dL	216	47.5 ± 10.9	45.8 ± 11.1	0.2
LDLc, mg/dL	216	118.9 (104.0, 141.9)	127.4 (106.9, 146.2)	0.12
ALT, U/L	216	32.1 (26.0, 41.2)	33.2 (25.9, 41.6)	0.7
AST, U/L	216	24.4 (20.0, 29.4)	24.1 (21.2, 30.6)	0.4
GGT, U/L	202	29.1 (20.2, 43.2)	31.8 (23.5, 39.6)	0.4
ALKP, mg/dL	216	71.8 (61.9, 83.8)	69.4 (60.1, 82.9)	0.5
hsCRP, mg/L	216	2.3 (1.3, 4.0)	2.5 (1.6, 4.3)	0.3
Positive APO-E[c]	214	20 (19.0 %)	15 (13.8 %)	0.3

ALT, Alanine Transaminase; ALKP, Alkaline Phosphatase; APO-E‡, Apolipoprotein E; AST, Aspartate Aminotransferase; BAG, brain age gap; CRP, C-reactive Protein; Diastolic BP, Diastolic blood pressure; GGT, gamma-glutamyl transferase; HbA1c, hemoglobin A1c; HDLc, high-density lipoprotein cholesterol; LDLc, low-density lipoprotein cholesterol; Systolic BP, Systolic blood pressure.

[a] Values are presented as either median (p25, p75), mean ± standard deviation for continuous variables, depending on their distribution, and as number (%) for categorical variables.

[b] Statistical tests used include Welch Two Sample t-test, Pearson's Chi-squared test, and Wilcoxon rank sum test.

[c] ApoE-ε4 was considered positive if there was 1 APOE-ε4 allele.

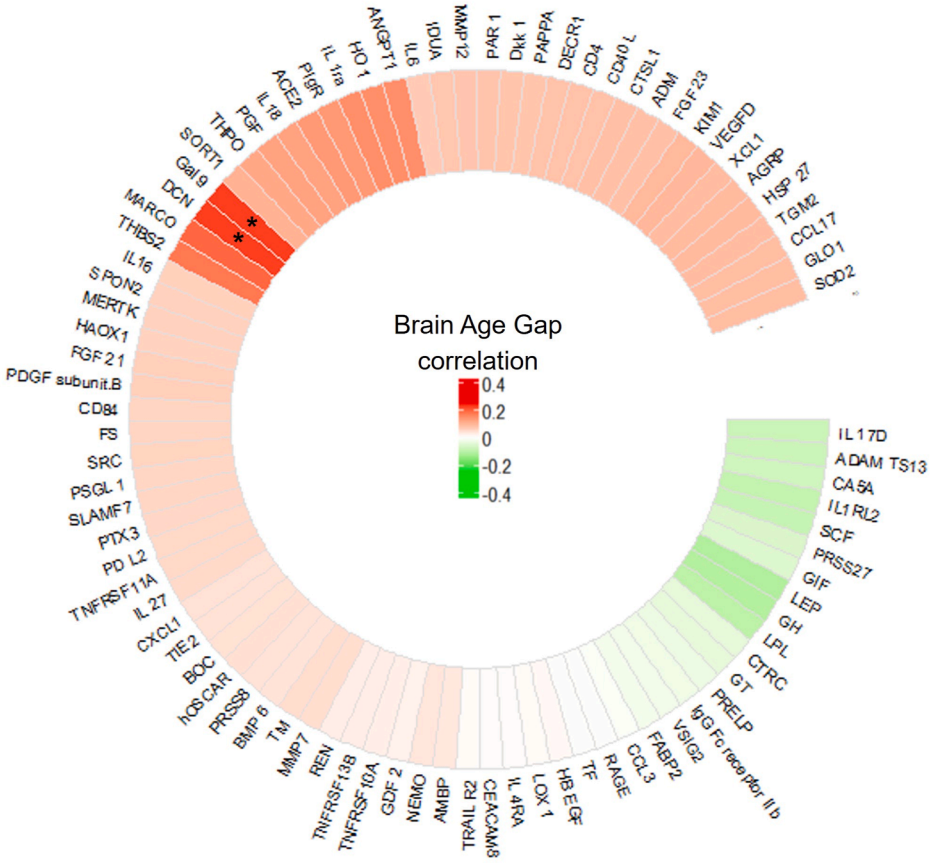

Fig. 2. Baseline correlation between Brain Age Gap and proteomic panel. Circular heatmap of the proteomic panel (N = 87 proteins). Spearman correlation test was used to test the correlations between baseline Brain Age Gap and each protein. Correlations adjusted for sex and age. * Denotes significant correlation at FDR <0.05 (N = 211).

sample size. Additional baseline-adjusted models incorporating lifestyle variables are provided in Supplementary Excel Table 1**.**

3.3. Proteomic score for brain age gap

Three models were utilized to determine whether proteomics significantly adds to other known or suspected markers to improve the prediction accuracy of BAG (Table 2, Supplementary Fig. 2). The first model (model i) only included the proteomic panel at baseline (87 proteins) and had an R squared (R^2) of 0.034 and root mean square error (RMSE) of 5.34. The 5 predictors of model i, according to their importance, were Gal-9, DCN, ANGPT1, THBS2, and LEP (Supplementary Fig. 2A). The second model (model ii) included only the traditional biomarkers at baseline (16 biomarkers: WC, BMI, systolic BP, diastolic BP, glucose, HbA1c, insulin, cholesterol, triglycerides, HDLc, low-density lipoprotein cholesterol (LDLc), alkaline phosphatase (ALKP), alanine transaminase (ALT), aspartate aminotransferase (AST), gamma-glutamyl transferase (GGT), c-reactive protein (CRP)) had an R^2 of 0.003 and RMSE of 67.75. The 6 predictors of model ii, according to importance, were WC, AST, SBP, DBP, ALKP, and HDLc (Supplementary Fig. 2B). The third model (model iii) tests whether a combination of the proteomic panel with traditional biomarkers would improve the prediction accuracy of BAG. This model yielded an R^2 of 0.041 and an RMSE of 5.16. The 10 first predictors of model 3, according to the importance, were Gal-9, DCN, MARCO, VEGFD, WC, PIgR, DBP, SBP, AST, ALKP, HDLc, ADAM-TS13, LEP (Supplementary Fig. 2C). Next, we validated the models presented in Table 2 on an 18-month time point from our DIRECT PLUS trial. Pearson R values for the validation sets were (model i, n = 210: r = 0.263; p = 1.09e-04, model ii, n = 213:

Table 2
Brain Age Gap prediction by the proteomic panel and traditional variables.

Type of models	Sample size	Number of predictors[a]	R2[b]	RMSE[b]
Model i: Panel proteomics only	206 observations	0-36 at each fold	0.034	5.34
Model ii: Traditional markers[c] only	188 observations	6-15 at each fold	0.003	66.75
Model iii: Panel proteomics with candidate[d] traditional markers	**205 observations**	**6–31 at each fold**	**0.041**	**5.16**

[a] Number of predictors in the last fold were further used to apply to the validation set: model i: Gal 9, DCN, ANGPT1, THBS2, LEP (5 proteins); model ii: WC, AST, SBP, DBP, ALKP, HDLc, (6 traditional markers); model iii: Gal-9, DCN, MARCO, VEGFD, WC, PIgR, DBP, SBP, AST, ALKP, HDLc, ADAM-TS13, LEP (6 traditional markers + 7 proteins).
[b] Considering all folds in LOOCV.
[c] List of traditional markers used in model ii: WC, BMI, systolic BP, diastolic BP, Glucose, HbA1c, Insulin, Cholesterol, Triglycerides, HDLc, LDLc, ALKP, ALT, AST, GGT, CRP.
[d] Significant markers from model ii were forced into model iii.

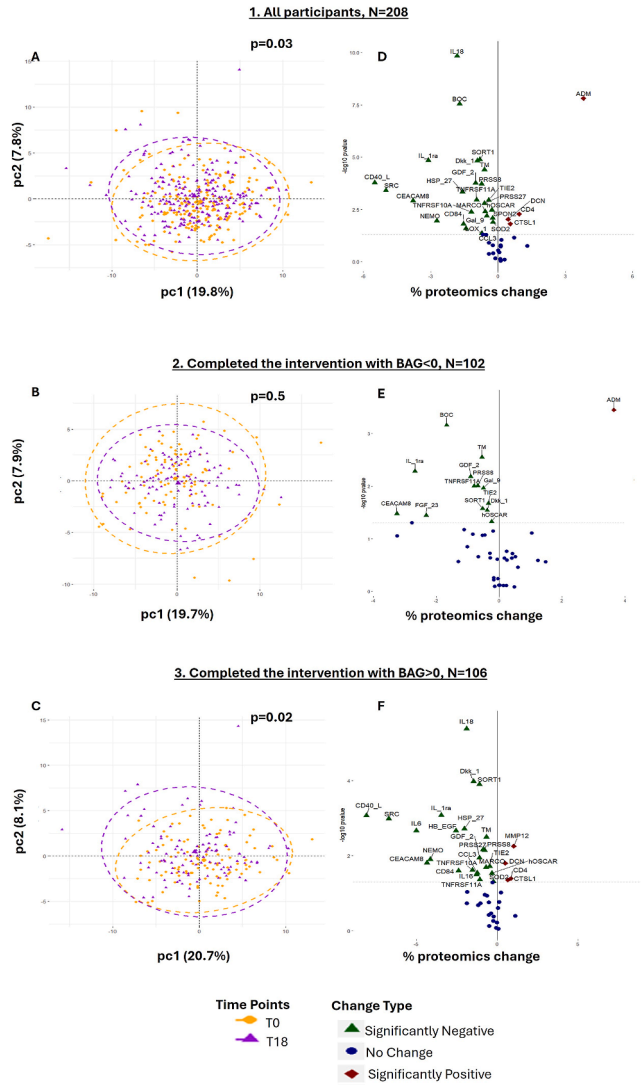

Fig. 3. Distinct Brain Age Gap switch groups and their proteomic phenotype. Panel 1. All participants, n = 208. Panel 2. Participants who completed with BAG<0, n = 102 (T0 + T18 with BAG <0 or T0 BAG >0 & T18 BAG<0). Panel 3. Participants who completed with BAG>0, n = 106 (T0 + T18 with BAG >0 or T0 BAG <0 & T18 BAG >0). PCA plots (A, B, C): PCA analysis for proteomics in distinct panel sub-groups, including baseline (T0) and 18-month time-points (T18). PC1 and PC2 are presented. P values for LMM between time points of PC1 are presented. Volcano plots (D, E, F): % proteomics change which correlated with PC1 (absolute correlation value > 0.1) was calculated relative to the baseline protein's expression. The statistical significance of the proteomics change (T18/T0) was analyzed using the Wilcoxon signed-rank test. The rhombus shape represents significant proteomics with a negative % change. The triangular shape represents significant proteomics with a positive % change. The circle shape represents non-significant proteomics.

r = 0.275; p = 4.76e-05, model iii, n = 210: r = 0.372; p = 3.52e-08, Supplementary Table 1).

3.4. Post-intervention distinct brain age gap groups and their proteomic phenotype

Next, we examined differences in the proteomics panel change between baseline and 18 months using PCA analysis for proteomics. Of the 216 participants with BAG, we had proteomics available for 208 at both time points (Fig. 3A). Using LMM, we found that the first principal component (PC1) was significantly different between the two-time points (p = 0.03). Further, we divided participants into two distinct groups of BAG change: participants who completed the 18-month intervention with negative BAG (younger brain than expected, N = 102) and participants who completed the intervention with positive BAG (older brain than expected, N = 106) (Fig. 3B-C). The PCA analysis for each group between the two-time points showed that PC1 was significantly different between the two-time point groups in participants who completed the intervention with an older brain than expected (p = 0.02). However, the difference was not significant in those who completed the intervention with a younger brain than expected (p = 0.5).

We further explored the individual proteins that most strongly predicted BAG change, with an absolute correlation higher than 0.1, for BAG change (for the proteomics panel list for each group, please see Supplementary Table 2). For all participants, we found significant positive and negative relative changes for DCN and Gal-9, respectively (Wilcoxon signed-rank test is applied, p < 0.05) (Fig. 3D; Supplementary Table 3). Our findings aligned with our initial results, a negative Gal-9 relative change to the baseline protein levels in participants who completed with a younger brain than expected and a positive DCN relative change to the baseline protein levels in participants who completed with a younger brain than expected (Fig. 3E-F; Supplementary Table 3; p < 0.05 for both).

3.5. Dynamics in Gal-9 and DCN levels in aging and diet groups

In the subsequent analysis, we examine whether specific age ranges exhibit a different level of DCN and Gal-9 markers, potential brain aging indicators. To this end, we conducted a quantile regression, dividing chronological age into quantiles and testing whether any quantile group displayed a significant correlation between age and DCN or Gal-9 markers (Fig. 4A-B).

We found a statistically significant association in the Gal-9 marker only among individuals of the highest age group (tau = 0.75, coefficients = 12.98, p < 0.001, mean age tertile = 63.7 years). Whereas, for DCN, a significant association was evident across all age groups, with a notably higher coefficient observed within the middle and higher quantiles (tau = 0.25, coefficients = 20.21, mean age tertile = 40.1 years, tau = 0.50, coefficients = 26.17, mean age tertile = 50.2 years, tau = 0.75, coefficients = 25.58, mean age tertile = 63.7 years, p < 0.001 for all; Table 3).

Using LMM, we also tested the interaction between the lifestyle intervention groups and the two-time points for the association with PC1. We found that the proteomics in the green-MED diet group showed a significant change during the intervention (β = −1.7; p of interaction = 0.05) compared to the HDG group. Finally, we quantified the specific change in DCN and Gal-9 biomarkers for each lifestyle intervention group. For Gal-9, the green-MED group experienced a mean ± se change of −0.104 ± 0.03, whereas Gal-9 changed only slightly in the MED (−0.03 ± 0.03) and HDG (0.002 ± 0.03) groups. Participants in the green-MED diet had a significant reduction in Gal-9 compared to the HDG diet after Bonferroni correction (p = 0.015), and only the green-MED diet had a significant reduction compared to the baseline (p = 0.003). Whereas green-MED, MED, and HDG diets represent the mean ± se DCN change of 0.008 ± 0.02, 0.039 ± 0.02, and 0.032 ± 0.013, respectively, with no significant difference between diets. In the HDG group, DCN tended to increase following the intervention compared to the baseline (p = 0.053) (Fig. 5).

We further explore whether the intake of specific polyphenol-rich foods could be associated with changes in Gal-9 levels over the intervention, as observed in the green-MED diet group. The results showed that: Green tea consumption of 4 cups per day was

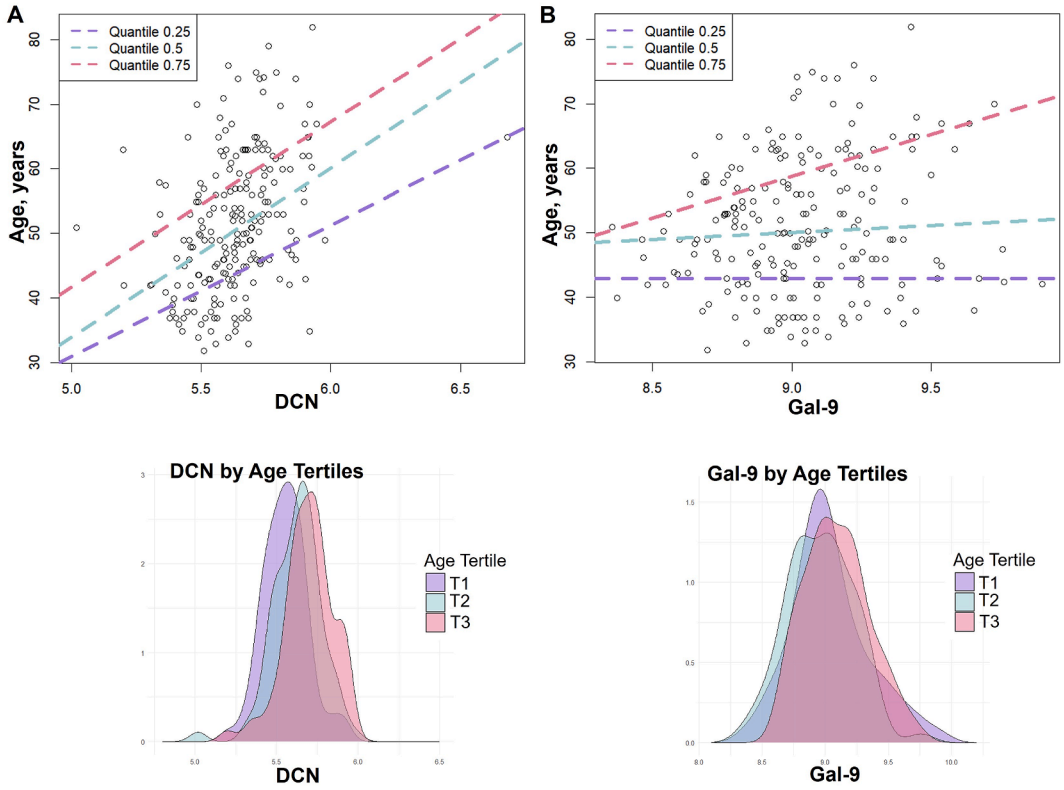

Fig. 4. Chronological age by the candidate proteins: DCN and Gal 9. Scatter plots of quantile regression at baseline and density plots of the candidate proteins by tertiles of chronological age. A. DCN; B. Gal-9.

Table 3
Quantile regression for prediction of chronological age by DCN and Gal-9.

Proteins	Y=Age at baseline	Tau = 0.25	Tau = 0.50	Tau = 0.75
Gal-9	Intercept	42.92	30.08	−58.00
	B	0	2.11	**12.98**[a]
DCN	Intercept	−69.98	−96.89	−86.21
	B	**20.21**[a]	**26.17**[a]	**25.58**[a]
	Mean tertile age (Years)[b]	40.1	50.2	63.7

[a] Denotes p < 0.05.
[b] Mean tertile groups (T1, T2, T3), density plots represent the Gal-9/DCN distribution across these tertiles.

significantly associated with a reduction in Gal-9 levels (β = −0.25, $p = 0.018$). In addition, consuming seven portions of walnuts per week was significantly associated with a reduction in Gal-9 levels (β = −0.20, $p = 0.0057$). However, consumption of seven Mankai shakes per week was associated with a reduction in Gal-9 levels (β = −0.21), although this association did not reach statistical significance (p = 0.20).

Finally, we pooled data from our two previous RCTs (DIRECT PLUS and CENTRAL) and examined whether baseline and post-intervention levels of DCN and Gal-9 could predict long-term cognitive function by Montreal Cognitive Assessment (MoCA) scores. We found that higher baseline levels of Gal-9 and DCN were significantly associated with lower cognitive performance (Gal-9: β = −1.34, p = 0.019; DCN: β = −3.46, p = 0.0005) after adjustment for age, sex, and trial. At 18 months post-intervention, the association remained significant for Gal-9 (β = −1.25, p = 0.035), while it was not significant for DCN (β = −1.16, p = 0.25).

4. Discussion

We found two specific serum protein expressions, Gal-9 and DCN, that reflect accelerated brain aging. These proteomic markers can improve the prediction of BAG together with traditional variables. We further showed that levels of Gal-9 and DCN might favorably be modified by the green-MED/high-polyphenol diet and that these changes are associated with better BAG. These findings are closely aligned with our previous results shadowing that the green-MED, high-polyphenol diet, rich in Mankai, green tea, and walnuts, and low in red/processed meat, is potentially neuroprotective for age-related brain atrophy [16].

Several limitations need to be acknowledged. First, the high proportion of male participants (90 %) may limit the generalizability of the findings to females. Additionally, the generalizability is further restricted since the participants had either abdominal obesity or dyslipidemia. Moreover, our proteomic assessment was limited to 87 proteins. In addition, this study lacks data about the participants' educational or cognitive status. Indeed, in contrast to the significant brain atrophy and MRI-based BAG changes by diet group, we previously reported that we could not detect significant cognitive function differences between the diet groups following the intervention, possibly due to the small sample size of the substudy, the limited sensitivity of the cognitive decline assessment methods or the short intervention time [16]. However, the objectively measured BAG indicates early signs of cognitive decline and AD [24–26].

Additionally, our analysis employed proteins from the Olink CVDII panel, which is not brain-specific. However, this panel was selected a priori based on its availability and relevance to the cardiometabolic focus of the original trial. Importantly, the panel includes numerous inflammatory and metabolic markers with

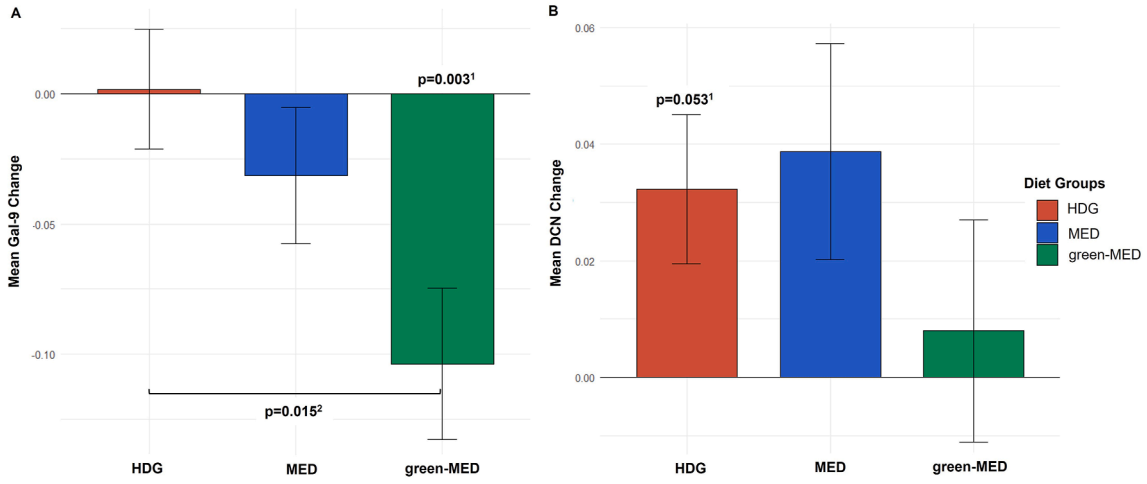

Fig. 5. 18-month changes in Gal-9 and DCN stratified by diet intervention groups. A: The Gal-9 mean ± SE changes are 0.002 ± 0.03 for HDG (n = 70), −0.03 ± 0.03 for Med (n = 70), and −0.104 ± 0.03 for Green Med (n = 76), respectively. B: The DCN mean ± SE changes are 0.008 ± 0.02, 0.039 ± 0.02, and 0.032 ± 0.013 for green-MED (n = 76), MED (n = 70), and HDG (n = 70), respectively. The mean and standard error are displayed on the graph for each group. "1"- p-value by LMM between time 0 and time 18 after Bonferroni correction. "2"- p-value between groups after Bonferroni correction.

recognized roles in neuroinflammation and brain aging, thereby offering a biologically plausible link to our secondary brain-related outcomes.

Also, in the elastic net analysis for model ii, we encountered 0 predictors across multiple folds during the training step. However, we intentionally used a rigorous model with BAG value as the dependent variable rather than just the brain age to remove the effect of chronological age. Although the proteomic model demonstrated improved predictive capacity for BAG compared to traditional cardiometabolic markers alone, the overall R^2 remained modest. Our primary aim was not to achieve optimal prediction accuracy but to assess the relative contribution of proteomic versus traditional variables, and to identify proteins most strongly associated with BAG. However, Gal-9 and DCN emerged consistently across elastic net models as top predictors, supporting their potential biological relevance. Finally, we did not conduct an external validation of the elastic net model for BAG prediction. Nonetheless, internal validation sets at time 18 showed significant results (Supplementary Table 1). The strengths of this study include a relatively large sample size, a high retention rate, long-term intervention, and using the gold-standard brain MRI measurements for brain age calculation [27,28].

In 1986, DCN was discovered to be a structural constituent of the extracellular matrix (ECM) [29]. Since then, the understanding of its role in various biological processes, including cell growth, differentiation, proliferation, and the regulation of inflammation and fibrillogenesis [30–32]. Higher levels of DCN in CSF are associated with early Aβ pathology. Increased CSF-DCN levels are present at an early stage of amyloid-β (Aβ) amyloidosis and correlate with core AD biomarkers such as CSF-Aβ42 and CSF-p-tau. Additionally, DCN has been found to activate neuronal autophagy by enhancing autophagosomal-lysosomal degradation, linking ECM changes to autophagy [33,34]. Moreover, DCN pathway is related to learning and recall in mice [35].

Gal-9 is a member of the family of galactoside-binding proteins. Among the galectin family members, galectins 1, 3, 4, 8, and 9 are significantly expressed in the brain and play crucial roles in neuromodulation, neuroinflammation, and neuroprotection [36]. Gal-9 has been implicated in the modulation of immune responses as it induces the release of proinflammatory cytokines, initiating an inflammatory cascade [37,38]. Moreover, recombinant Gal-9 suppresses T lymphocytes but induces oligodendrocyte maturation and myelin repair in mixed glial cultures [39]. Also, Gal-9 is expressed in astrocytes of multiple sclerotic lesions in the CSF of patients with multiple sclerosis [40]. Furthermore, both ileal bile acid binding protein (I-BABP) and Gal-9 levels were elevated in AD patients [41]. Gal-9 exerts pro-inflammatory effects in the brain by binding to the Tim-3 receptor on microglia, leading to increased production of cytokines such as IL-6, factors known to exacerbate neurodegeneration in AD [42]. Experimental models suggest that blocking the Gal-9/Tim-3 signaling pathway may protect hippocampal integrity and enhance cognitive function in response to amyloid β (Aβ) exposure [43]. Recent findings demonstrate that Gal-9 plays a role in immune evasion by malignant cells, supporting their survival and suppressing anti-tumor immunity [44]. Moreover, Gal-9 is expressed in cells of both the innate and adaptive immune system, and has been implicated in the development of immune-related diseases such as tumor immune escape and chronic inflammation [45].

Furthermore, elevated circulating levels of Gal-9 have been associated with both MCI and progression toward AD [41]. Similarly, Gal-3, another member of the galectin family (not included in our proteomic panel), is expressed in microglia clustered around Aβ plaques, particularly in the hippocampus, compared to the frontal cortex in AD patients. Higher Gal-3 levels are correlated with tau and p-Tau181 levels, two indicators of pathology progression in AD [46,47].

In our study, we conducted stratified analyses according to APOE-ε4 carrier status. Although within each genotype subgroup, the associations between Gal-9 and DCN with BAG did not remain statistically significant after FDR correction, the correlation coefficients and their confidence intervals were similar to those observed in the full cohort. Based on the existing literature, a potential genetic explanation related to APOE-ε4 can be proposed, which may be linked to the associations observed between DCN, Gal-9, and BAG. Prior research has shown that APOE-ε4 carriers have neuroinflammatory responses, potentially mediated by increased microglial activation and elevated pro-inflammatory cytokine production, which may underlie their greater exposure to neurodegeneration [48]. Gal-9 and its receptor, Tim-3, are upregulated in activated microglia and have been implicated in modulating neuroinflammation, including in models of

amyloid–β–induced [42]. While direct mechanistic links between APOE-ε4 and Gal-9 remain to be elucidated, experimental evidence suggests that Gal-9 may act downstream of APOE-related inflammatory pathways [49]. In addition, recent single-cell RNA sequencing studies have shown that DCN is upregulated in endothelial and fibroblast cell clusters responsive to peripheral APOE-ε4 expression, particularly in the context of inflammation-associated angiogenesis [50].

Participants in the green-MED diet had a reduction in Gal-9 as compared to the HDG, and only the green-MED diet group had a significant reduction compared to the baseline. DCN increased in all diet groups, but least (not statistically significant) in the green-MED group. We previously reported that the green-MED (high-polyphenol) diet, rich in Mankai, green tea, walnuts, and low in red/processed meat, is potentially neuroprotective for age-related brain atrophy [16]. The polyphenols in this diet may play a role in neuroprotection by reducing microglial activation, which is a key driver of neuroinflammation in the central nervous system. These polyphenols, such as EGCG compounds, have been shown to reduce neuroinflammation and attenuate amyloid β accumulation, mechanisms involved in brain aging [51,52]. These neuroprotective effects may offer a plausible mechanistic explanation for the observed reduction in Gal-9, a pro-inflammatory marker, and the attenuated increase in DCN in the green-MED group.

In conclusion, by integrating proteome-wide screening with focused hypothesis-driven inquiry, our analytical framework effectively balanced discovery and validation, while controlling for multiple comparisons. The consistency of diet-related effects on DCN and Gal-9 across models highlights their promise as responsive indicators for nutritional interventions aimed at healthy cognitive aging. Future work should expand these findings in diverse populations and explore whether changes in DCN and Gal-9 predict long-term cognitive outcomes. Overall, these results advance our understanding of how dietary strategies influence molecular mechanisms underlying brain aging. The study supports the potential of the green-MED diet as a non-pharmacological approach to slow or prevent age-related neurobiological decline.

Author contribution

AYM, ER, GT, HZ, AK, and IShai conceptualized the DIRECT PLUS and performed the data collection. DP and AYM performed the statistical analysis, interpreted the data, reviewed the literature, and drafted the manuscript. AK performed the MRI-based brain analysis. GL and OF calculate the brain age. IShelef supervised the MRI acquisition. KN performed the proteomic measurements. BI and UC analyzed the data. IShai is the principal investigator of the DIRECT PLUS trial. All authors contributed to the interpretation of data and reviewed this work's language and intellectual content. MStumvoll, FB, VW, TRR, MB, MSalti, FBH, DDW, MJS, I Shelef, GA, and IShai revised the final draft of the study and approved the final version. No one who meets the criteria for authorship has been omitted from the author list.

Data availability

All data described in the article, code book, and analytic code will be made available upon request, pending the approval of the principal investigator (irish@bgu.ac.il).

Ethical approval

The study was approved by the Institutional Review Board at Soroka University Medical Center (approval number SOR-0280-16) and was registered at ClinicalTrials.gov (NCT03020186). All participants provided written informed consent.

Funding

Funding: This study was supported by the German Research Foundation (DFG) project number 209933838 (SFB 1052; B11) (to I Shai); the Israel Ministry of Health grant 87472511 (to I Shai); the Israel Ministry of Science and Technology grant 3-13604 (to I Shai); and the California Walnut Commission (to I Shai). DP is a recipient of the Kreitman Doctoral Fellowship at the Ben-Gurion University of the Negev. AYM was supported by the Council for Higher Education- Zuckerman support program for outstanding postdoctoral female researchers. None of the funding providers were involved in any stages of the design, conducting, or analysis of the study, nor did they have access to the study results prior to publication.

Declaration of competing interest

The authors declare the following financial interests/personal relationships which may be considered as potential competing interests: Matthias Bluher received honoraria for lectures and consultancy from Amgen, Astra Zeneca, Bayer, Boehringer-Ingelheim, Lilly, Novartis, Novo Nordisk, and Sanofi. If there are other authors, they declare that they have no known competing financial interests or personal relationships that could have appeared to influence the work reported in this paper.

Acknowledgments

We would like to thank Dr. Assaf Rudich from the Ben-Gurion University of the Negev. We thank the DIRECT PLUS participants for their valuable contributions. We thank MRI technician Eli Atyia and the team from the Nuclear Research Center Negev; Efrat Pupkin, Eyal Goshen, Avi Ben Shabat, and Evyatar Cohen for their valuable contributions to this study.

Appendix A. Supplementary data

Supplementary data to this article can be found online at https://doi.org/10.1016/j.clnu.2025.08.021.

References

[1] Schuff N, Tosun D, Insel PS, Chiang GC, Truran D, Aisen PS, et al. Nonlinear time course of brain volume loss in cognitively normal and impaired elders. Neurobiol Aging 2012;33:845–55.
[2] Callisaya ML, Beare R, Moran C, Phan T, Wang W, Srikanth VK. Type 2 diabetes mellitus, brain atrophy and cognitive decline in older people: a longitudinal study. Diabetologia 2019;62:448–58.
[3] Enzinger C, Fazekas F, Matthews P, Ropele S, Schmidt H, Smith S, et al. Risk factors for progression of brain atrophy in aging: six-year follow-up of normal subjects. Neurology 2005;64:1704–11.
[4] Janelidze S, Mattsson N, Palmqvist S, Smith R, Beach TG, Serrano GE, et al. Plasma P-tau181 in Alzheimer's disease: relationship to other biomarkers, differential diagnosis, neuropathology and longitudinal progression to Alzheimer's dementia. Nat Med 2020;26:379–86.
[5] van Gennip AC, Stehouwer CD, van Boxtel MP, Verhey FR, Koster A, Kroon AA, et al. Association of type 2 diabetes, according to the number of risk factors within target range, with structural brain abnormalities, cognitive performance, and risk of dementia. Diabetes Care 2021;44:2493–502.
[6] Nakamura A, Kaneko N, Villemagne VL, Kato T, Doecke J, Doré V, et al. High performance plasma amyloid-β biomarkers for Alzheimer's disease. Nature 2018;554:249–54.
[7] Pachter D, Kaplan A, Tsaban G, Zelicha H, Meir AY, Rinott E, et al. Glycemic control contributes to the neuroprotective effects of mediterranean and green-mediterranean diets on brain age; the DIRECT PLUS Brain-MRI randomized controlled trial. Am J Clin Nutr 2024;120(5):1029–36.
[8] Lampe L, Zhang R, Beyer F, Huhn S, Kharabian Masouleh S, Preusser S, et al. Visceral obesity relates to deep white matter hyperintensities via inflammation. Ann Neurol 2019;85:194–203.

[9] Kerti L, Witte AV, Winkler A, Grittner U, Rujescu D, Flöel A. Higher glucose levels associated with lower memory and reduced hippocampal microstructure. Neurology 2013;81:1746–52.
[10] Hofmann SM, Beyer F, Lapuschkin S, Goltermann O, Loeffler M, Müller K-R, et al. Towards the interpretability of deep learning models for multi-modal neuroimaging: finding structural changes of the ageing brain. Neuroimage 2022;261:119504.
[11] Leonardsen EH, Vidal-Piñeiro D, Roe JM, Frei O, Shadrin AA, Iakunchykova O, et al. Genetic architecture of brain age and its casual relations with brain and mental disorders. Mol Psychiatr 2023:1–10.
[12] Cole JH, Franke K. Predicting age using neuroimaging: innovative brain ageing biomarkers. Trends Neurosci 2017;40:681–90.
[13] Franke K, Gaser C. Ten years of BrainAGE as a neuroimaging biomarker of brain aging: what insights have we gained? Front Neurol 2019:789.
[14] Cole JH, Poudel RP, Tsagkrasoulis D, Caan MW, Steves C, Spector TD, et al. Predicting brain age with deep learning from raw imaging data results in a reliable and heritable biomarker. Neuroimage 2017;163:115–24.
[15] Baecker L, Garcia-Dias R, Vieira S, Scarpazza C, Mechelli A. Machine learning for brain age prediction: introduction to methods and clinical applications. EBioMedicine 2021;72.
[16] Kaplan A, Zelicha H, Yaskolka Meir A, Rinott E, Tsaban G, Levakov G, et al. The effect of a high-polyphenol mediterranean diet (Green-MED) combined with physical activity on age-related brain atrophy: the dietary intervention randomized controlled trial polyphenols unprocessed study (DIRECT PLUS). Am J Clin Nutr 2022;115:1270–81.
[17] Levakov G, Kaplan A, Meir AY, Rinott E, Tsaban G, Zelicha H, et al. The effect of weight loss following 18 months of lifestyle intervention on brain age assessed with resting-state functional connectivity. eLife 2023;12:e83604.
[18] Meir AY, Rinott E, Tsaban G, Zelicha H, Kaplan A, Rosen P, et al. Effect of green-Mediterranean diet on intrahepatic fat: the DIRECT PLUS randomised controlled trial. Gut 2021;70:2085–95.
[19] Shai I, Schwarzfuchs D, Henkin Y, Shahar DR, Witkow S, Greenberg I, et al. Weight loss with a low-carbohydrate, mediterranean, or low-fat diet. N Engl J Med 2008;359:229–41.
[20] Gepner Y, Golan R, Harman-Boehm I, Henkin Y, Schwarzfuchs D, Shelef I, et al. Effects of initiating moderate alcohol intake on cardiometabolic risk in adults with type 2 diabetes: a 2-year randomized, controlled trial. Ann Intern Med 2015;163:569–79.
[21] Kaplan A, Zelicha H, Tsaban G, Meir AY, Rinott E, Kovsan J, et al. Protein bioavailability of Wolffia globosa duckweed, a novel aquatic plant–A randomized controlled trial. Clin Nutr 2019;38:2576–82.
[22] Yaskolka Meir A, Tuohy K, von Bergen M, Krajmalnik-Brown R, Heinig U, Zelicha H, et al. The metabolomic-gut-clinical axis of mankai plant-derived dietary polyphenols. Nutrients 2021;13:1866.
[23] Sela I, Yaskolka Meir A, Brandis A, Krajmalnik-Brown R, Zeibich L, Chang D, et al. Wolffia globosa–mankai plant-based protein contains bioactive vitamin B12 and is well absorbed in humans. Nutrients 2020;12:3067.
[24] Millar PR, Gordon BA, Luckett PH, Benzinger TL, Cruchaga C, Fagan AM, et al. Multimodal brain age estimates relate to Alzheimer disease biomarkers and cognition in early stages: a cross-sectional observational study. eLife 2023;12:e81869.
[25] Doering E, Antonopoulos G, Hoenig M, van Eimeren T, Daamen M, Boecker H, et al. MRI or 18F-FDG PET for brain age gap estimation: links to cognition, pathology, and Alzheimer disease progression. J Nucl Med 2024;65:147–55.
[26] Dohm-Hansen S, English JA, Lavelle A, Fitzsimons CP, Lucassen PJ, Nolan YM. The'middle-aging'brain. Trends Neurosci 2024;47(4):259–72.
[27] Finkelstein O, Levakov G, Kaplan A, Zelicha H, Meir AY, Rinott E, et al. Deep learning-based BMI inference from structural brain MRI reflects brain alterations following lifestyle intervention. Hum Brain Mapp 2024;45:e26595.
[28] Levakov G, Rosenthal G, Shelef I, Raviv TR, Avidan G. From a deep learning model back to the brain—Identifying regional predictors and their relation to aging. Hum Brain Mapp 2020;41:3235–52.
[29] Krusius T, Ruoslahti E. Primary structure of an extracellular matrix proteoglycan core protein deduced from cloned cDNA. Proc Natl Acad Sci 1986;83:7683–7.
[30] Ruoslahti E, Yamaguchi Y. Proteoglycans as modulators of growth factor activities. Cell 1991;64:867–9.
[31] Yamaguchi Y, Ruoslahti E. Expression of human proteoglycan in Chinese hamster ovary cells inhibits cell proliferation. Nature 1988;336:244–6.
[32] Yamaguchi Y, Mann DM, Ruoslahti E. Negative regulation of transforming growth factor-β by the proteoglycan decorin. Nature 1990;346:281–4.
[33] Jiang R, Smailovic U, Haytural H, Tijms BM, Li H, Haret RM, et al. Increased CSF-decorin predicts brain pathological changes driven by Alzheimer's Aβ amyloidosis. Acta Neuropathol Commun 2022;10:96.
[34] Jiang R, Smailovic U, Haytural H, Haret R, Shevchenko G, Tijms B, et al. Decorin is an early CSF biomarker of Alzheimer's Aβ amyloidosis. Alzheimer's association international conference: ALZ. 2021.
[35] Ma N, You C, Geng S, Zhao S, Ren H, Zheng L. Effect of growth associated Protein-43-Mediated regulation of the Decorin/Lysine oxidase pathway on learning and memory ability in alzheimer's disease model mice. Nanosci Nanotechnol Lett 2020;12:612–8.
[36] da Rosa MM, de Aguiar Ferreira M, de Oliveira Lima CA, Mendonça ACS, Silva YM, Sharjeel M, et al. Alzheimer's disease: is there a role for galectins? Eur J Pharmacol 2021;909:174437.
[37] Premeaux TA, D'Antoni ML, Abdel-Mohsen M, Pillai SK, Kallianpur KJ, Nakamoto BK, et al. Elevated cerebrospinal fluid Galectin-9 is associated with central nervous system immune activation and poor cognitive performance in older HIV-infected individuals. J Neurovirol 2019;25:150–61.
[38] Steelman AJ, Li J. Astrocyte galectin-9 potentiates microglial TNF secretion. J Neuroinflammation 2014;11:1–12.
[39] Li Y-H, Zhou W-H, Tao Y, Wang S-C, Jiang Y-L, Zhang D, et al. The Galectin-9/Tim-3 pathway is involved in the regulation of NK cell function at the maternal–fetal interface in early pregnancy. Cell Mol Immunol 2016;13:73–81.
[40] Burman J, Svenningsson A. Cerebrospinal fluid concentration of Galectin-9 is increased in secondary progressive multiple sclerosis. J Neuroimmunol 2016;292:40–4.
[41] Wang X, Niu Y, Yue C-x, Fu S, Wang R-t. Increased ileal bile acid binding protein and galectin-9 are associated with mild cognitive impairment and Alzheimer's disease. J Psychiatr Res 2019;119:102–6.
[42] Hernández ER, Zimbrón LFH, Pérez ES, Salgado JLS, Morales MAP, Zenteno E. Galectin-9 and Tim-3 are upregulated in response to microglial activation induced by the peptide Amyloid-β (25–35). Neuropeptides 2024;105:102426.
[43] Zhang G, Peng Q, Guo X, Pan L, Xiong M, Zhang X, et al. Microglia-derived Galectin-9 drives amyloid-β pathology in Alzheimer's disease. Aging Cell 2025:e14396.
[44] Yıldırım C. Galectin-9, a pro-survival factor inducing immunosuppression, leukemic cell transformation and expansion. Mol Biol Rep 2024;51:571.
[45] Cao Z, Leng P, Xu H, Li X. The regulating role of galectin-9 in immune cell populations. Front Pharmacol 2024;15:1462061.
[46] Boza-Serrano A, Vrillon A, Minta K, Paulus A, Camprubí-Ferrer L, Garcia M, et al. Galectin-3 is elevated in CSF and is associated with Aβ deposits and tau aggregates in brain tissue in Alzheimer's disease. Acta Neuropathol 2022;144:843–59.
[47] García-Revilla J, Boza-Serrano A, Espinosa-Oliva AM, Soto MS, Deierborg T, Ruiz R, et al. Galectin-3, a rising star in modulating microglia activation under conditions of neurodegeneration. Cell Death Dis 2022;13:628.
[48] Safieh M, Korczyn AD, Michaelson DM. ApoE4: an emerging therapeutic target for Alzheimer's disease. BMC Med 2019;17:1–17.
[49] Krautter F, Hussain MT, Zhi Z, Lezama DR, Manning JE, Brown E, et al. Galectin-9: a novel promoter of atherosclerosis progression. Atherosclerosis 2022;363:57–68.
[50] Liu C-C, Zhao J, Fu Y, Inoue Y, Ren Y, Chen Y, et al. Peripheral apoE4 enhances Alzheimer's pathology and impairs cognition by compromising cerebrovascular function. Nat Neurosci 2022;25:1020–33.
[51] Rezai-Zadeh K, Shytle D, Sun N, Mori T, Hou H, Jeanniton D, et al. Green tea epigallocatechin-3-gallate (EGCG) modulates amyloid precursor protein cleavage and reduces cerebral amyloidosis in Alzheimer transgenic mice. J Neurosci 2005;25:8807–14.
[52] Youn K, Ho C-T, Jun M. Multifaceted neuroprotective effects of (-)-epigallocatechin-3-gallate (EGCG) in Alzheimer's disease: an overview of preclinical studies focused on β-amyloid peptide. Food Sci Hum Wellness 2022;11:483–93.